

Paweł GIL¹

MORPHOLOGY OF SYNTHETIC JET

Synthetic jet devices consist of an oscillating driver, a cavity, and a small opening such as a circular, square or rectangular orifice. When the driver is oscillating, it produces a series of vortex rings at the orifice. The device generates the zero net mass flux (ZNMF) because the identical fluid mass and the mass flow are sucked and flowed out across the orifice. Although there is no net mass transfer to its surroundings, the ZNMF device has the interesting property of causing a finite amount of momentum transfer to its surroundings. The experimental result of synthetic jet flow visualization is presented in this paper. Synthetic jet visualization is carried out using smoke visualization with light sheet. Five qualitatively different flow field regimes were identified, depending upon the Reynolds and Stokes number. Vortex ring generation and propagation are also presented and analyzed in this paper.

Keywords: synthetic jet, vortex ring, morphology, vortex generation, coherent structure

1. Introduction

A zero net mass flux (ZNMF) device consists of an oscillating driver attached in some manner to a cavity that contains an orifice. This driver may be, for example a speaker, piezoelectric diaphragm or a mechanical piston. The driver has the effect of periodically increasing and decreasing the volume of the cavity. This motion can cause fluid to be alternately expelled and ingested through the orifice.

Figure 1 illustrates a typical ZNMF device being operated to produce a synthetic jet. If the driver amplitude ② is high enough, as fluid is expelled through the orifice ③, the boundary layer separates from the wall and, at edge of the orifice, rolls up to produce a vortex ring ⑤. A vortex ring propagates away from the orifice under its own self-induced velocity. During the subsequent suction stroke, the fluid is drawn into the cavity from the surrounding ④, but the vortex ring ⑤ moves sufficiently far from the orifice ③ so as to be relatively unaffected. A new vortex rings are then ejected and the cycle continues, producing a train of vortex rings.

¹ Autor do korespondencji/corresponding author: Paweł Gil, Politechnika Rzeszowska, Wydział Budowy Maszyn i Lotnictwa, Zakład Termodynamiki, al. Powstańców Warszawy 8, 35-959 Rzeszów, e-mail: gilpawel@prz.edu.pl

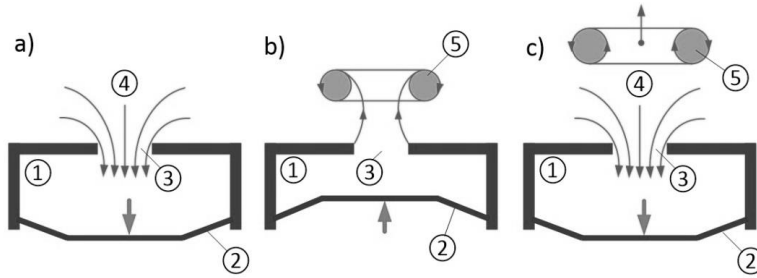


Fig. 1. The formation and evolution of synthetic jet: a) suction stroke, b) producing a vortex ring during ejection stroke c) suction stroke, vortex ring propagates away from the orifice. ① - cavity, ② - diaphragm, ③ - orifice, ④ - fluid, ⑤ - vortex ring

Although acoustic driven flows has been investigated since the 1950s by Ingard and Labate [11], the first synthetic jet generator was most likely a laboratory air-jet generator designed and used by Dauphinee [2]. Since the end of the last century, the synthetic jet has been the subject of both experimental and numerical investigations, usually under the name SJ (“synthetic jet”) [12, 13, 15] or ZNMF (“zero net mass flux”) [1, 17]. Synthetic jet considered to be a relatively new technology has a great potential in many practical applications, especially for the purpose of flow manipulation [8, 14] as well as heat transfer enhancement [5, 7]. It has been well established that the two most critical parameters required to characterize a synthetic jet flow are the Reynolds number, and the dimensionless stroke length or inverse Strouhal number [6, 10].

Shuster et al. [18] undertook a comprehensive investigation of a free synthetic jet flow field utilizing PIV. A lot of data were presented detailing the evolution of the jet, however, with dimensionless stroke lengths between $1 \leq L \leq 3$ and various Reynolds numbers. A number of other authors including Glezer [9], Didden [3] and Gharib et al. [4] have presented data on the formation and evolution of vortex rings which are concerned exclusively with individual rings rather than an established flow. McGuinn et al. [16] identifies the various flow regimes as a function of dimensionless stroke length in the range of $3 \leq L \leq 32$ and single Reynolds numbers $Re = 1500$.

The aim of this study is to identify a synthetic jet flow regime as a function of Reynolds number and for single Stokes number for a wide range of dimensionless number $0 \leq Re \leq 3340$ and $0 \leq L \leq 6.9$. Also the aim of this work is to determine the formation criterion for a synthetic jet and the identification of the region in terms of best heat dissipation.

2. Experimental setup

The synthetic jet actuator designed for the purpose of the present study is shown in Fig. 2. It consists of an actuator (loudspeaker STX W.18.200.8.FGX) of 0.15 m diameter as the vibrating element fitted to a plexiglas plate having

a centered bore of 0.15 m. The loudspeaker nominal impedance is 8Ω and nominal resonance frequency is 37 Hz. The sheets are fastened using four bolts. The depth of the cavity H can be adjusted by adding (or removing) plexiglas plates with 0.15 m bore in between. Experiments are carried out for single orifice diameters $d = 0.024$ m, for single orifice lengths $t = 0.005$ m, and for single cavity depths $H = 0.06$ m. Working fluid is air. The coordinate system is presented in Fig. 2. Note that x is axial and r is radial coordinate. All connections between sheets and the loudspeaker have been sealed with silicone paste for the purpose of the leakages elimination.

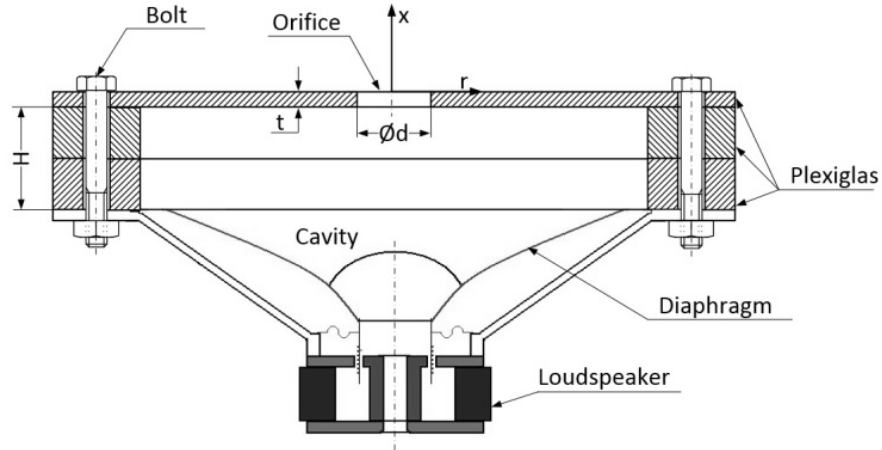


Fig. 2. Schematic of synthetic jet actuator

A digital sinusoidal signal generated from LabVIEW application is converted to analog signal with 16-bit 48 kHz Realtek ALC889 DAC (Digital to Analog Converter). The LM3886 Texas Instruments amplifier is used to amplify an analog signal from DAC and to excite the actuator.

Multifunction board (Keithley KPCI-3116A) is used for the purpose of continuous monitoring of the actuator input. The measurement of current in conjunction with voltage gives electrical power supplied to the loudspeaker. The output voltage from the actuator is maintained constant for a particular set of experiments. The sampling frequencies of current and voltage measurements are 32 times the actuator excitation frequency.

A constant temperature of hot-wire anemometer (HPA 98 The Strata Mechanics Research Institute) with tungsten–platinum coated single wire probe of sensing element length 0.001 m is used for the velocity measurements. During the calibration conducted in the low-speed wind tunnel of Rzeszow University of Technology [19], the reference velocity was measured with a Pitot tube connected to the pre-calibrated FirstSensor HCLA differential pressure transducer. Measurement points are fitted with a 6th order polynomial curve with a maximum error of 2%. The hot-wire probe is mounted on a two-dimensional manipu-

lator, which allows positioning the probe with an accuracy of $1 \cdot 10^{-5}$ m. The measurements are taken at orifice radial coordinate ranging from $r = 0$ to $d/2$ and 0.001 m away from the orifice plate in the axial direction x (Fig. 3). Although we are aware that the measurements should ideally be taken at $x = 0$ m, such a procedure turned out to be infeasible due to the hazard of the destruction of hot-wire probe. The constant temperature of hot-wire anemometer was connected to the multifunction board (Keithley KPCI-3116A). The sampling frequency was at least 32 times the excitation frequency for all velocity measurements, so for actuator frequency 2Hz sampling frequency was 64 samples per second. Synthetic jet flow visualization setup utilizes synthetic jet actuator with glycerin vapor generator inside and light sheet (Fig. 4).

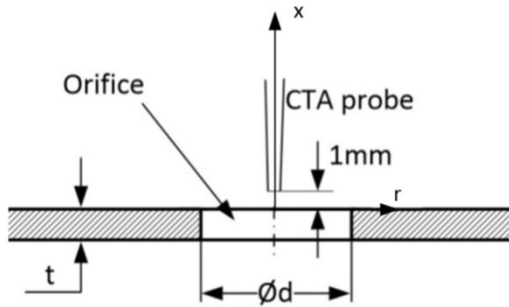


Fig. 3. Hot wire (CTA) position with respect to synthetic jet generator orifice exit

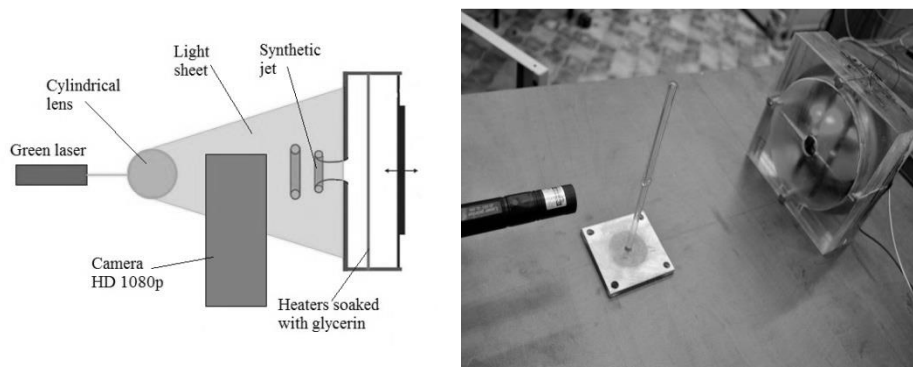


Fig. 4. Synthetic jet flow visualization setup: schematic (left), photo (right)

Glycerin vapor generator consists of two heaters installed in the cavity of synthetic jet actuator connected to DC power supply. The heaters are soaked with glycerin. The electrical current raises the temperature of the heater causing the evaporation of glycerin. In order to improve visualization of synthetic jet flow, it was decided to highlight glycerin vapor with light sheet. Green laser

with a wavelength of 532 nm and 10 mW, and a cylindrical lens having a diameter of 0.006 m were used to produce light sheet. The angle of propagation of the light sheet was about 70°. Image was captured with a digital camera with a resolution of 1920x1080 HD and 24 frames per second.

3. Dimensionless number

The synthetic jet Reynolds number is calculated using the procedure given by Holman et al. [10] based on spatial and time-averaged exit velocity during the ejection stroke:

$$Re = \frac{U \cdot d}{\nu} \quad (1)$$

where: U – characteristic velocity defined as:

$$U = \frac{2}{T} \cdot \frac{1}{A} \int_A \int_0^{\tau/2} (u) d\tau dA \quad (2)$$

where: T – period, A – orifice area, u – instantaneous velocity, τ – time, d – orifice diameter, ν – kinematic viscosity.

The synthetic jet Stokes number:

$$Stk = \sqrt{\frac{2\pi f d^2}{\nu}} \quad (3)$$

where: f – oscillation frequency.

The inverse Strouhal number:

$$\frac{1}{Sh} = \frac{U}{2\pi f d} = \frac{Ud/\nu}{2\pi f d^2/\nu} = \frac{Re}{Stk^2} \quad (4)$$

Dimensionless stroke lengths:

$$L = \pi \frac{Re}{Stk^2} = \frac{\pi}{Sh} \quad (5)$$

Physically a stroke length is a distance that a fluid particle travels near the surface of the orifice during a cycle. Current measurements were performed for the following parameter listed in table 1. Synthetic jet flow visualization covers the range up to $x/d = 6$.

Table 1. Range of tested parameters

d [m]	t [m]	H [m]	x/d [-]	f [Hz]	Re [-]	Stk [-]	L [-]
0.024	0.005	0.06	0÷6	2	0	22	0.00
0.024	0.005	0.06	0÷6	2	280	22	0.58
0.024	0.005	0.06	0÷6	2	364	22	0.75
0.024	0.005	0.06	0÷6	2	418	22	0.86
0.024	0.005	0.06	0÷6	2	449	22	0.93
0.024	0.005	0.06	0÷6	2	620	22	1.28
0.024	0.005	0.06	0÷6	2	1600	22	3.30
0.024	0.005	0.06	0÷6	2	2234	22	4.62
0.024	0.005	0.06	0÷6	2	3340	22	6.90

4. Results

Synthetic jet flow visualization shows the process of generating vortex ring (Fig. 5). If the loudspeaker diaphragm amplitude is high enough, as fluid is expelled through the orifice, the boundary layer separates from the wall (Fig. 5b, c) and, at edge of the orifice, rolls up to produce a vortex ring (Fig. 5d, e). A vortex ring propagates away from the orifice under its own self-induced velocity (Fig. 5e, f). Five regions of jet synthetic jet flow regimes based on the synthetic jet flow visualization at a constant Stokes number and a variable Reynolds number were identified schematically presented in Fig. 6 and table 2.

First regime (Fig. 6a) - no synthetic jet. Fluid is drawn into and expelled from the cavity under low amplitude of diaphragm oscillation. This condition prevents rolling of fluid into coherent vortex. The synthetic jet does not occur.

Second regime (Fig. 6b) - the transition region. The vortex rolls up entirely close to the edge of the orifice. Momentum transferred to the vortex is too small, the vortex cannot propagate under the self-induced velocity. However, in the suction stroke vortex is sucked into cavity. This regime is characterized by the continuous production and destroying of vortex ring.

Third regime (Fig. 6c) - weak synthetic jet. The vortex rolls up at a certain distance from the edge of the nozzle $x/d = 0.5$ to 1.5 . The vortex is pushed out from the orifice but the vortex has too small momentum to propagate under self-induced velocity. This causes the effect of spinning vortex in situ. Synthetic jet reaches distances up to $x/d \approx 3$.

Fourth region (Fig. 6d) - coherent vortex ring has a momentum large enough to propagate under the self-induced velocity. Vortex quickly escapes from the orifice vicinity.

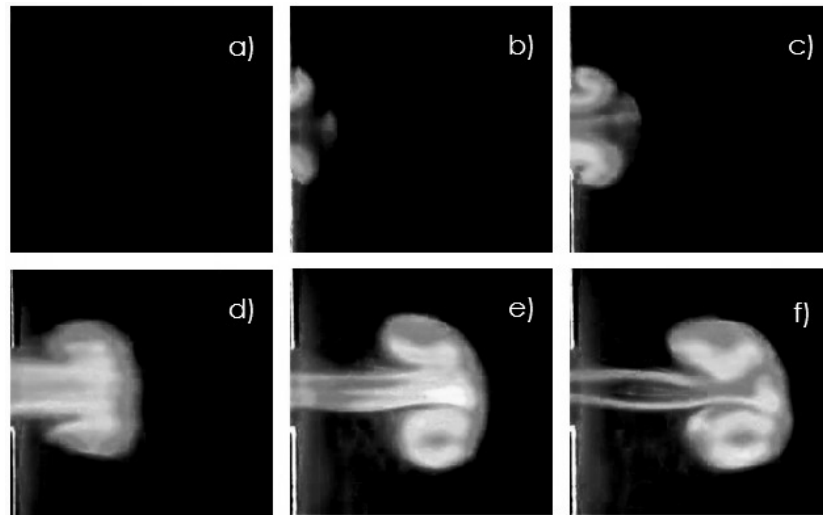


Fig. 5. Synthetic jet flow visualization – generating of vortex ring: a) ejection stroke begins, b) fluid is expelled through the orifice, the fluid separates from the edge of the orifice, c) rolling fluid into vortex ring, d) the ejected fluid from the cavity pushes vortex ring out of the orifice, e) vortex ring is formed, f) propagation of vortex ring

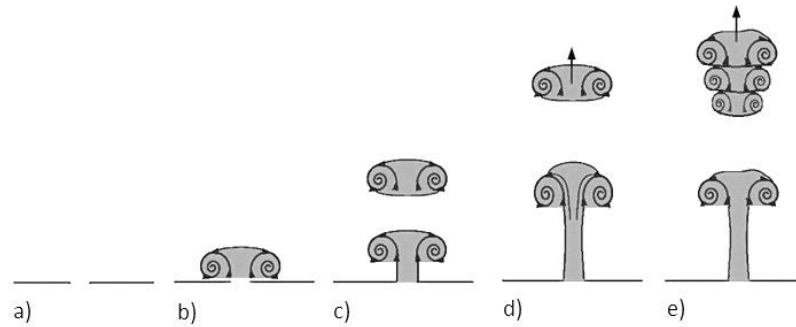


Fig. 6. Morphology of synthetic jet

Table 2. Morphology of synthetic jet

Name (Fig. 6)	L	Description
Regime a)	< 0.82	No jet
Regime b)	$0.82 \div 2.36$	The transition region, suction of the vortex ring to the cavity
Regime c)	$2.36 \div 3.14$	Weak synthetic jet, coherent vortex ring revolves in situ
Regime d)	$3.14 \div 4.71$	Synthetic jet, vortex ring propagates away from the orifice under its own self-induced velocity
Regime e)	> 4.71	Strongly turbulent synthetic jet

Fifth regime (Fig. 6e) - vortex ring is rapidly discharged together with the air from the orifice. The rush of air from the orifice is large enough to cause instability of the initial vortex ring which is not able to store all the energy in its vortices. Primary vortex breaks into few secondary vortices. It created a highly turbulent synthetic jet.

5. Summary

Synthetic jet flow visualization revealed the process of generation of vortex ring and motion of this coherent structure in the near field. Synthetic jet flows are mainly characterized by the Reynolds number and Stokes number. Five synthetic jet flow morphology regimes are identified and based on threshold values of dimensionless stroke lengths L . Formation criterion for synthetic jet was assumed to be $L = 0.82$ (between regimes a) and b) presented in Fig. 6) which is in a good agreement with literature [10, 20]. The morphology of synthetic jet is important in choosing appropriate flow regime for the heat transfer enhancement. The best regime in terms of heat dissipation appears to be regime d) and e) because of highly turbulent flow and long-range interaction. The synthetic jet flow visualization will be conducted for different Stokes number to investigate influence on synthetic jet flow and morphology.

References

- [1] Cater J.E., Soria J.: The evolution of round zero-net-mass-flux jets, *J. Fluid Mech.* 472 (2002), 167-200.
- [2] Dauphinee T.M.: Acoustic air pump, *Rev. Sci. Instrum.* 28 (6) (1957), 456.
- [3] Didden N.: On the formation of vortex rings: rolling-up and production of circulation, *ZAMP*, 30 (1979) 101-116.
- [4] Gharib M., Rambod E., Shariff K.: A universal time scale for vortex ring formation, *J. Fluid Mech.*, 360 (1998), 121-140.
- [5] Gil P., Smusz R., Strzelczyk P.: Badania eksperymentalne wymiany ciepła przy wykorzystaniu strugi syntetycznej. *Termodynamika i wymiana ciepła w badaniach procesów cieplno-przepływowych*. OW PRz, Rzeszów 2014, ss. 187-198.
- [6] Gil P., Strzelczyk P.: Performance and efficiency of loudspeaker driven synthetic jet actuator, *Exp. Therm. Fluid Sci.*, 76 (2016), 163-174.
- [7] Gil P., Strzelczyk P.: Porównanie właściwości chłodzących strugi syntetycznej i strugi swobodnej, *ZN PRz Mechanika* 87 (2015), 105-117.
- [8] Gil P.: Przejście strugi syntetycznej w strugę turbulentną, *ZN PRz Mechanika*, 88 (2016), 37-46.
- [9] Glezer A.: The formation of vortex rings, *Phys. Fluids*, 31 (1988), 3532-3542.
- [10] Holman R., Utturkar Y., Mittal R., Smith B.L., Cattafesta L.: Formation criterion for synthetic jets, *AIAA J.*, 43 (2005), 2110-2117.
- [11] Ingard U., Labate S.: Acoustic circulation effects and the nonlinear impedance of orifices, *J. Acoust. Soc. Am.* 22 (1950), 211-218.

- [12] Jain M., Puranik B., Agrawal A.: A numerical investigation of effects of cavity and orifice parameters on the characteristics of a synthetic jet flow, *Sens. Actuators, A* 165 (2011) 351-366.
- [13] James R.D., Jacobs J.W., Glezer A.: A round turbulent jet produced by an oscillating diaphragm, *Phys. Fluids*, 8 (1996), 2484-2495.
- [14] Li Y., Bai H., Gao N.: Drag of a D-shaped bluff body under small amplitude harmonic actuation, *Theor. Appl. Mech. Letters*, 5 (2015) 35-38.
- [15] Mallinson S.G., Reizes J.A., Hong G.: An experimental and numerical study of synthetic jet flow, *Aeronaut. J.*, 105 (2001) 41-49.
- [16] McGuinn A., Farrelly R., Persoons T., Murray D. B.: Flow regime characterization of an impinging axisymmetric synthetic jet, *Exp. Therm. Fluid Sci.*, 47 (2013), 241-251.
- [17] Pack L.G., Seifert A.: Periodic excitation for jet vectoring and enhanced spreading, *J. Aircraft*, 38 (2001) 486-495.
- [18] Shuster J.M., Smith D.R.: Experimental study of the formation and scaling of a round synthetic jet, *Phys. Fluids*, 19 (2007) 045109.
- [19] Strzelczyk P.: Tunel aerodynamiczny do badania śmigieł, *J. Aeronautica Integra*, 1 (2006) 69-72.
- [20] Travnicek Z., Broucková Z., Kordík J.: Formation criterion for axisymmetric synthetic jets at high Stokes numbers. *AIAA J.*, 50 (2012) 2012-2017.

MORFOLOGIA STRUGI SYNTETYCZNEJ

Streszczenie

Generator strugi syntetycznej składa się z elementu drgającego, komory oraz okrągłej, prostokątnej lub kwadratowej dyszy. Podczas oscylacji generatora wytwarzana jest seria wirów pierścieniowych na krawędzi dyszy. Urządzenie to generuje zerowy strumień masowy w przekroju dyszy, ponieważ identyczna masa płynu jest zasysana i wyrzucana przez dyszę. Pomimo tego, że strumień masowy wynosi zero to generator strugi syntetycznej powoduje niezerową zmianę pędu płynu, który to w pewnej odległości od dyszy wywołuje przepływ (strugę syntetyczną). W artykule zaprezentowano wynik badań eksperymentalnych wizualizacji przepływu strugi syntetycznej. Wizualizacja strugi syntetycznej została przeprowadzona przy wykorzystaniu dymu oraz płaszczyzny świetlnej. Zidentyfikowano pięć jakościowo różnych regionów strugi syntetycznej w zależności od liczb Reynoldsa oraz Stokesa. W artykule zaprezentowano i przeanalizowano również mechanizm tworzenia i rozprzestrzeniania się wirów pierścieniowych.

Słowa kluczowe: struga syntetyczna, wir pierścieniowy, morfologia, powstawanie wiru, struktura koherentna

DOI: 10.7862/rm.2017.15

Otrzymano/received: 22.03.2017

Zaakceptowano/accepted: 14.05.2017

